Organization and Dynamics of NBD-Labeled Lipids in Membranes Analyzed by Fluorescence Recovery after Photobleaching

Thomas J. Pucadyil,† Soumi Mukherjee, and Amitabha Chattopadhyay*

Centre for Cellular and Molecular Biology, Uppal Road, Hyderabad 500 007, India

Received: September 18, 2006; In Final Form: January 5, 2007

Lateral diffusion of membrane constituents plays an important role in membrane organization and represents a central theme in current models describing the structure and function of biological membranes. Fluorescence recovery after photobleaching (FRAP) is a widely used approach that provides information regarding dynamic properties and spatial distribution of membrane constituents. On the basis of the unique concentration-dependent fluorescence emission properties of a fluorescently labeled cholesterol analogue modified at the tail region, 25-[*N*-[(7-nitrobenz-2-oxa-1,3-diazol-4-yl)-methyl]amino]-27-norcholesterol (25-NBD-cholesterol), we have previously shown that it exhibits local organization even at very low concentrations in membranes. In this paper, we address aspects regarding the molecular size and dynamics of such an organized assembly of 25-NBD-cholesterol by monitoring its lateral diffusion characteristics using FRAP. To obtain a comprehensive understanding of the organization and dynamics of 25-NBD-cholesterol in the membrane, we compare its diffusion properties to that of a fluorescent phospholipid analogue 1,2-dipalmitoyl-*sn*-glycero-3-phosphoethanolamine-*N*-(7-nitro-2-(1,3-benzoxadiazol-4-yl)) (NBD-PE). Our results indicate significant differences in the membrane dynamics of these NBD-labeled lipids. Importantly, on the basis of a novel wavelength-selective FRAP approach, our results show that the organization of 25-NBD-cholesterol is heterogeneous, with the presence of fast- and slow-diffusing species which could correspond to predominant populations of monomers and dimers of 25-NBD-cholesterol. The potential application of the wavelength-selective FRAP approach to monitor the organization and dynamics of molecules in membranes therefore represents an exciting possibility.

Introduction

Biological membranes are complex assemblies of lipids and proteins that allow cellular compartmentalization and act as the interface through which cells communicate with each other and with the external milieu. The heterogeneous distribution of membrane constituents is responsible for diversity in the membrane environment. Lipids in model and biological membranes are often found distributed nonrandomly in domains or pools. Such distribution has been attributed to the unique packing preferences of lipids which are intrinsically determined by their structures and/or their interactions with neighboring molecules. For instance, the unique chemical structures of lipids such as cholesterol[1,2] and phosphatidylethanolamine[3,4] distinct from phosphatidylcholine which comprise the bulk of the membrane and electrostatic interactions between proteins and phosphatidylinositols[5] contribute to their sorting in membranes giving rise to regions relatively enriched in such lipids. The segregation of membrane lipids in domains assumes importance due to their regulatory role in cellular functions such as membrane sorting and signal transduction.[6,7] In this regard, the further development of nonperturbing approaches that quantitatively analyze the organization of membrane constituents assumes significance.[8]

Spectroscopic and microscopic techniques applied to fluorescent lipid analogues represent a powerful set of approaches for monitoring membrane organization due to their high sensitivity, time resolution, and multiplicity of measurable parameters.[9−13] Lipids covalently linked to extrinsic fluorophores are commonly used for such studies. The advantage with this approach is that one has a choice of the fluorescent label to be used, and therefore, specific probes with appropriate characteristics can be designed for specific applications. A widely used extrinsic fluorophore in biophysical, biochemical, and cell biological studies is the 7-nitrobenz-2-oxa-1,3-diazol-4-yl (NBD) group (reviewed in ref 12). The NBD moiety possesses some of the most desirable properties for serving as an excellent probe for both spectroscopic and microscopic applications.[12,13] The fluorescent derivative of cholesterol, 25-[*N*-[(7-nitrobenz-2-oxa-1,3-diazol-4-yl)methyl]amino]-27-norcholesterol or 25-NBD-cholesterol, in which the NBD group is attached to the flexible alkyl chain of cholesterol (see Figure 1a), represents one such example. The detailed characterization of the spectroscopic properties of 25-NBD-cholesterol in model membranes and membrane-mimetic systems has been previously reported.[14−19] The NBD group in this analogue has been found to be localized deep in the hydrocarbon region of the membrane, approximately 5−6 Å from the center of the bilayer, thereby indicating that the orientation of this analogue in the membrane is similar to that of cholesterol.[14,15] It has also previously been shown by electrophoretic measurements that 25-NBD-cholesterol is not charged when bound to membranes at neutral pH.[15] Interestingly, unlike phospholipids labeled in their acyl chains, the NBD group in 25-NBD-cholesterol has been shown not to loop back to the membrane interface possibly due to the stereochemical rigidity of the sterol ring and/or the reduction of hydrophilicity due to the methyl group (not present in NBD-labeled phospho-

* To whom correspondence should be addressed. Tel.: +91-40-2719-2578. Fax: +91-40-2716-0311. E-mail: amit@ccmb.res.in.

† Present address: Room MB114, Department of Cell Biology, The Scripps Research Institute, La Jolla, CA 92037.

10.1021/jp066092h CCC: $37.00
Published on Web 02/08/2007

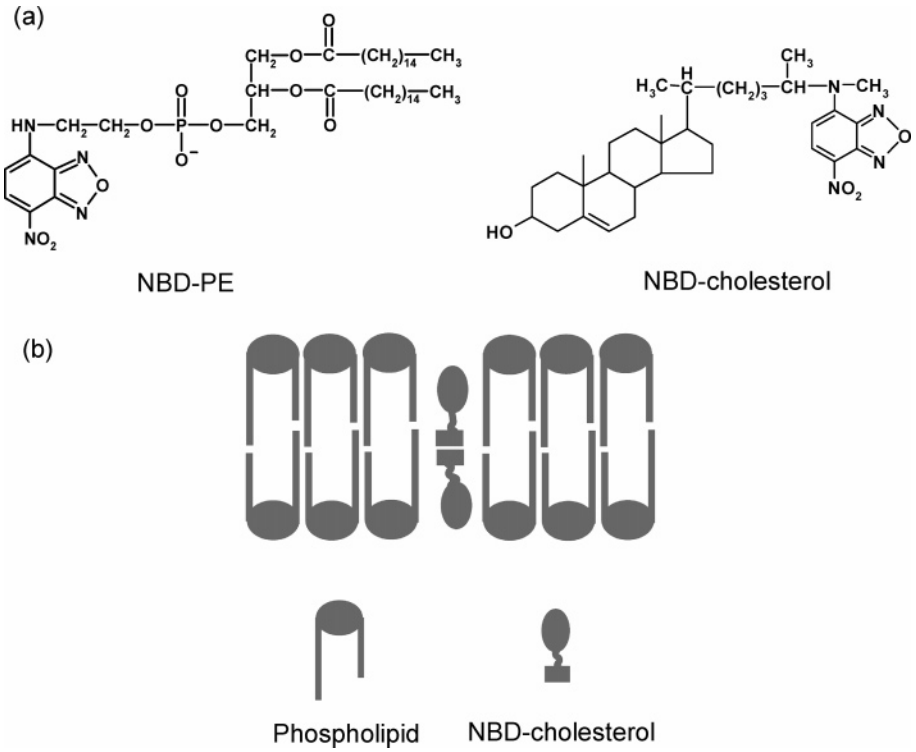

Figure 1. (a) Chemical structures of NBD-labeled cholesterol and phospholipid analogues, 25-NBD-cholesterol and NBD-PE. (b) Schematic diagram of the membrane bilayer showing the transbilayer tail-to-tail dimers of 25-NBD-cholesterol in membranes at low concentrations (reproduced from ref 16).

lipids) attached to the NBD moiety.[12] This unique orientation of 25-NBD-cholesterol offers a convenient means to localize a polar and potentially reactive group deep inside the membrane. Moreover, the unique position of this probe in the membrane has previously been exploited in fluorescence resonance energy transfer experiments to study the spatial orientation of specific sites on the chloroplast coupling factor in the membrane in reconstituted vesicles thereby providing further support for its orientation.[20]

We have previously monitored the organization of 25-NBD-cholesterol in membranes.[16,17,19] These results indicated that, at low concentrations, 25-NBD-cholesterol exhibits a unique organization possibly in the form of transbilayer tail-to-tail dimers that span the bilayer (see Figure 1b). In addition, we showed that the transbilayer dimer arrangement of 25-NBD-cholesterol observed at low concentrations is sensitive to membrane curvature and is stringently controlled by a narrow window of membrane thickness thereby reinforcing the transbilayer (rather than lateral) nature of the dimer.[17] Importantly, these results are supported by similar observations with native cholesterol using calorimetric approaches[21] and with dehydroergosterol, a naturally occurring fluorescent cholesterol analogue, using fluorescence spectroscopy.[17,22] Taken together, these observations collectively emphasize the existence of a transbilayer organization of 25-NBD-cholesterol at low concentrations in the membrane. While these experiments have provided valuable insight into the organization of 25-NBD-cholesterol at low concentrations in the membrane, aspects related to the molecular size and lateral diffusion of such an organized assembly of 25-NBD-cholesterol and their residence time in the membrane remain unexplored.

Lateral diffusion of membrane constituents plays an important role in membrane organization and represents a central theme in current models describing the structure and function of biological membranes.[8,23,24] Fluorescence recovery after photobleaching (FRAP) is a widely used approach that provides information regarding dynamic properties and spatial distribution of membrane constituents.[8] Furthermore, the analysis of lateral diffusion of membrane constituents by FRAP provides a global perspective regarding membrane organization relevant to most biological processes since its temporal and spatial resolution are generally in the seconds and micrometer range. In this paper, we monitored the lateral diffusion characteristics of 25-NBD-cholesterol using FRAP to gain further insight into the local organization it exhibits in membranes. Further, we compared dynamics of 25-NBD-cholesterol to that of phospholipids, which typically represent bulk membrane constituents, using a fluorescent phospholipid analogue 1,2-dipalmitoyl-*sn*-glycero-3-phosphoethanolamine-*N*-(7-nitro-2-(1,3-benzoxadiazol-4-yl) (NBD-PE). The NBD group in NBD-PE is attached to the headgroup of a phosphatidylethanolamine molecule (see Figure 1a). Interestingly, our results show that the organization of 25-NBD-cholesterol at low concentrations in such membranes is heterogeneous and different from bulk phospholipids, with the presence of fast- and slow-diffusing populations which could correspond to the monomer and the previously proposed[16,17] transbilayer tail-to-tail dimers of 25-NBD-cholesterol.

It must be mentioned here that the presence of a large and polar NBD group in 25-NBD-cholesterol buried deep in the membrane bilayer would quite obviously perturb membrane physical properties thereby limiting its use as a bulk cholesterol analogue at high concentrations. This is apparent from the reduced ability of 25-NBD-cholesterol to condense phospholipid fatty acyl chains compared to native cholesterol at high concentrations (20 mol %)[25] and the sorting out of 25-NBD-cholesterol in membranes existing in a cholesterol-rich, liquid-ordered phase.[26] The use of 25-NBD-cholesterol to analyze membrane organization of molecules using FRAP in this study is therefore prompted by the unique concentration-dependent spectroscopic properties exhibited by this molecule (see above).

Experimental Section

Materials. Dipalmitoyl-*sn*-glycero-3-phosphocholine (DPPC) and 25-NBD-cholesterol were obtained from Avanti Polar Lipids (Birmingham, AL). NBD-PE was from Molecular Probes (Eugene, OR). Cholesterol was from Sigma Chemicals Co. (St. Louis, MO). The purity of these lipids and fluorescent analogues was checked by thin layer chromatography on precoated silica gel plates from Merck (Darmstadt, Germany) with the solvent system of chloroform/methanol/water (65:25:4, v/v/v). All lipids and fluorescent analogues were found to give only one spot upon charring with a solution of cupric sulfate (10%, w/v) and phosphoric acid (8%, v/v) at 150 °C thereby confirming their purity. Water was purified through a Millipore (Bedford, MA) Milli-Q system and used throughout. The concentration of DPPC was determined by phosphate assay subsequent to total digestion by perchloric acid.[27] Lipid digestion was assessed using 1,2-dimyristoyl-*sn*-glycero-3-phosphocholine (DMPC) as an internal standard. The concentrations of 25-NBD-cholesterol and NBD-PE in methanol were calculated from their molar absorption coefficients (ϵ) of 22 000 M^{-1} cm^{-1} at 484 nm[17] and 21 000 M^{-1} cm^{-1} at 463 nm,[28] respectively.

Sample Preparations. Samples containing 495 nmol of DPPC and 5 nmol of 25-NBD-cholesterol or 490 nmol of DPPC, 5 nmol of cholesterol, and 5 nmol of NBD-PE were mixed in methanol and dried under a stream of nitrogen while being warmed gently (~35 °C). The small amount (1 mol %) of cholesterol was included in multilamellar vesicles prepared with NBD-PE as a control for the vesicles containing 25-NBD-cholesterol. The lipids were further dried under high vacuum for at least 3 h and hydrated (swelled) with 0.5 mL of water maintained at 60 °C (i.e., well above the phase transition temperature of DPPC) while being vortexed vigorously for 3 min to generate multilamellar vesicles. Vesicles prepared in this manner were incubated at 60 °C for 3 h and were then kept at room temperature (~23 °C) in the dark for 2 days for equilibration before making measurements. All measurements were performed at 23 °C which ensures that DPPC is in the gel phase. It must be mentioned here that equilibration of multilamellar vesicles was critical in achieving reproducibility in the concentration-dependent shifts in fluorescence emission of 25-NBD-cholesterol as well as in lateral diffusion measurements of fluorescent analogues using FRAP.

Fluorescence Spectroscopy. Steady-state fluorescence measurements were performed on a Hitachi F-4010 spectrofluorometer using 1-cm path length quartz cuvettes. Excitation and emission slits with a nominal bandpass of 5 nm were used for all measurements. The excitation wavelength used was 488 nm in all cases. Background intensities of samples in which the fluorescent probes were omitted were subtracted from each sample spectrum to cancel out any contribution of the solvent Raman peak and other scattering artifacts. All experiments were done with multiple sets of samples.

Confocal Microscopy and FRAP Experiments. Multilamellar vesicles prepared as described above were concentrated by low-speed centrifugation followed by resuspension of the pellet in a small volume of water. An aliquot (~5 μL) of this solution was sandwiched between a clean glass slide and a coverslip, and the edges of the coverslip were sealed with nail enamel. Fluorescence images of multilamellar vesicles that were ~20 μm or larger in diameter were acquired on an inverted Zeiss LSM 510 Meta confocal laser scanning microscope (Jena, Germany), with a 63×, 1.2 NA water-immersion objective using the 488 nm line of an argon laser as the excitation source. Fluorescence emission was collected using the Zeiss LSM Meta detector that provides a minimum spectral resolution of 10.7 nm. Fluorescence emission of 25-NBD-cholesterol and NBD-PE were acquired at a wavelength range of 505−558 nm using the Meta detector. For wavelength-selective FRAP experiments, fluorescence emission of 25-NBD-cholesterol was simultaneously acquired at the two wavelength ranges (505−526, 537−558 nm) using the Meta detector. All images were acquired with the pinhole set to 1 airy unit and at 512 × 512 pixel resolution. Qualitative FRAP experiments involved imaging the entire equatorial section of an isolated multilamellar vesicle, bleaching a circular region of interest of 1.75 μm radius within the vesicle, and monitoring fluorescence recovery kinetics into the bleached spot by imaging the entire vesicle. Scanning parameters were optimized by such qualitative FRAP experiments to avoid photobleaching of samples due to repeated imaging. This was assessed by monitoring the fluorescence intensity in regions of the multilamellar vesicle outside the bleached region for the entire duration of a FRAP experiment. Quantitative FRAP experiments performed at a higher temporal resolution involved restricting the area scanned and photobleached to a circular region of 1.75 μm radius within the multilamellar vesicle. Background fluorescence intensity was determined by performing the same experiment on an area on the coverslip devoid of vesicles. The mean postbleach fluorescence intensity in the circular region was background subtracted and normalized to the mean prebleach intensity. The fluorescence recovery kinetics was analyzed to determine the characteristic diffusion time (τ_d) on the basis of a model describing fluorescence recovery into a uniformly bleached circular disk:[29]

$$F(t) = [F(\infty) - F(0)][\exp(-2\tau_d/t)(I_0(2\tau_d/t) + I_1(2\tau_d/t))] + F(0) \quad (1)$$

Here $F(t)$ is the mean background corrected and normalized fluorescence intensity at time t in the circular region of interest, $F(\infty)$ is the recovered fluorescence intensity at time $t = \infty$, and $F(0)$ is the bleached fluorescence intensity at time $t \rightarrow 0$. I_0 and I_1 are modified Bessel functions. The bleach time point was calculated as the midpoint of the bleach duration. This resulted in the first normalized postbleach time point starting from a time $t > 0$. Curve fitting to eq 1 involved constraining the parameters $F(0) \geq 0$ and $F(\infty) \leq 1$. Fluorescence recovery data that showed systematic deviation from the fitted plots possibly due to physical displacement of the vesicle during the experiment were discarded. The diffusion coefficient (D) was determined from the equation

$$D = \omega^2/4\tau_d \quad (2)$$

where ω is the radius of the circular region of interest. Mobile fraction estimates of the fluorescence recovery were calculated according to the equation

$$\text{mobile fraction} = [F(\infty) - F(0)]/[F(p) - F(0)] \quad (3)$$

where $F(p)$ is the mean background corrected and normalized prebleach fluorescence intensity. Nonlinear curve fitting of the fluorescence recovery data to eq 1 and statistical analysis to determine significance levels by one-way ANOVA were carried out with Graphpad Prism software version 4.00 (San Diego, CA). For representation purposes, fluorescence recovery data in Figures 4 and 7 have been normalized according to $[F(t) - F(0)]/[F(p) - F(0)]$.

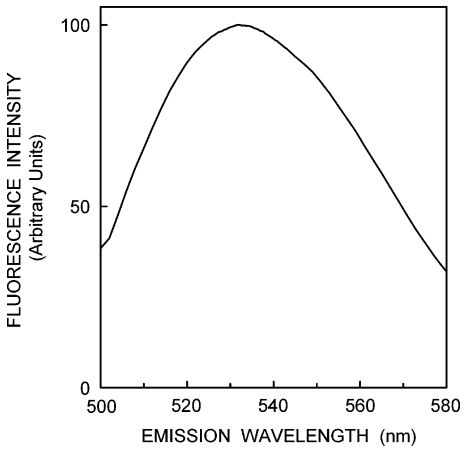

Figure 2. Fluorescence emission spectrum of 1 mol % NBD-PE in multilamellar vesicles of DPPC in the gel phase. The concentration of DPPC was 300 μM, and the excitation wavelength was 488 nm. See Experimental Section for other details.

Results

The organization of 25-NBD-cholesterol at low concentrations has previously been characterized in detail in gel phase DPPC membranes using fluorescence spectroscopy.[16,17,19] An independent, diffusion-based approach to analyze such organization in gel phase DPPC membranes could therefore corroborate the results obtained earlier using fluorescence spectroscopy. Furthermore, sensitive detection of a population of molecules on the basis of their size using FRAP appears to be possible only in gel phase membranes.[30] This is due to the fact that the dependence of lateral mobility of small molecules on their size has been observed only in gel phase membranes and has been attributed to the constraints imposed on displacement of molecules due to the enhanced order in gel phase membranes (see later). We therefore performed FRAP experiments with 25-NBD-cholesterol in gel phase DPPC membranes. The FRAP approach involves generating a concentration gradient of fluorescent molecules by irreversibly photobleaching a fraction of fluorophores in the observation region. The dissipation of this gradient with time owing to diffusion of fluorophores into the bleached region from the neighboring unbleached regions in the membrane is an indicator of the mobility of fluorophores in the membrane. We chose to use multilamellar vesicles for FRAP measurements due to their large size which allows their visualization in a microscopic field and the relative ease with which they can be prepared from a variety of lipids.[31,32] The large size of the vesicles is also useful in restricting their movement during experiments involving time-lapse imaging.

To obtain a comprehensive understanding of the organization and dynamics of cholesterol at low concentrations, we first analyzed the lateral diffusion behavior of phospholipids in gel phase DPPC membranes using NBD-PE with di16:0 fatty acyl chains (Figure 1a). The fluorescence emission spectrum of NBD-PE in such vesicles (Figure 2) appears smooth and homogeneous with a peak centered at 532 nm, in agreement with the previously reported value.[33] These vesicles appear large and uniformly fluorescent when observed under the confocal microscope (see Figure 3a). Figure 3 shows a representative FRAP experiment performed on such vesicles. The scanning parameters for all FRAP experiments were optimized to ensure no significant fluorescence photobleaching due to repeated imaging. This is indicated by the relatively constant mean fluorescence intensity in region 2 of the vesicle for the entire duration of the experiment (see Figure 3b). Nonlinear curve

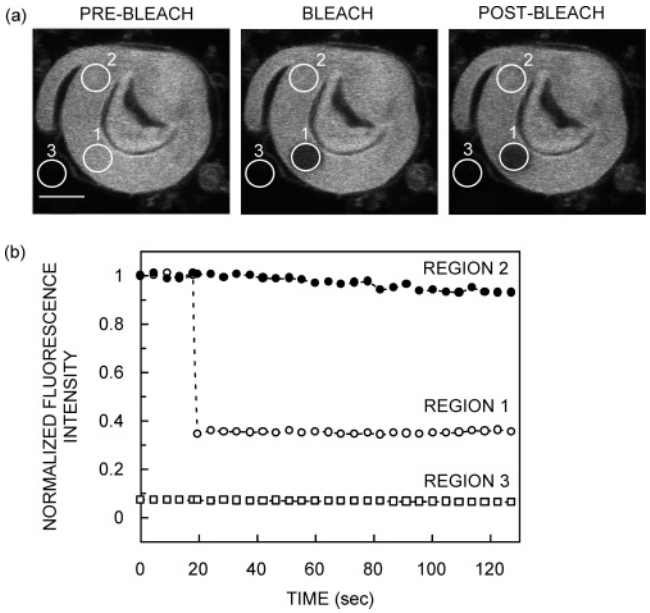

Figure 3. Representative FRAP measurement performed on a DPPC multilamellar vesicle containing NBD-PE. Panel a represents confocal sections of a DPPC multilamellar vesicle containing NBD-PE at 1 mol % concentration. The excitation wavelength was 488 nm, and fluorescence emission was collected from 505 to 558 nm. Fluorescence images of the same vesicle were acquired before bleach (prebleach), immediately after bleach (bleach), and after recovery of fluorescence (postbleach). The circular region 1 represents the bleached spot, region 2 reports fluorescence intensity outside the bleached spot but within the vesicle, and region 3 reports background fluorescence intensity. Panel b represents fluorescence intensity in the regions indicated in panel a over the entire time period of the FRAP experiment. Data corresponding to the mean normalized fluorescence intensity in regions 1−3 of panel a are shown in panel b. The mean fluorescence intensities represented in panel b have been normalized to the prebleach intensities in the respective region of interest and to the intensity in region 1. The almost constant fluorescence intensity in region 2 indicates no significant photobleaching in the field due to repeated imaging in spite of the relatively slow diffusion in gel phase membranes. The scale bar represents 5 μm. See the Experimental Section for other details.

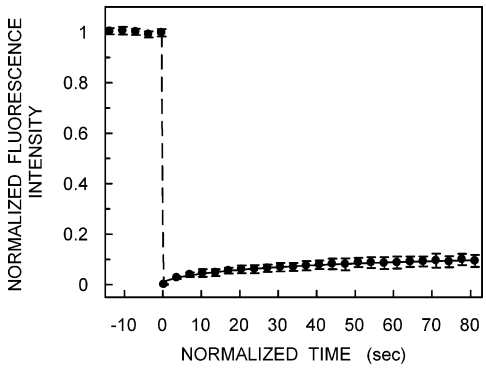

Figure 4. FRAP recovery kinetics of NBD-PE in DPPC multilamellar vesicles. The excitation wavelength was 488 nm, and fluorescence emission was collected from 505 to 558 nm. The normalized prebleach intensities are shown at time $t < 0$. The solid lines are nonlinear regression fits to the experimental data using eq 1. The data represent means ± standard deviations of several independent experiments (on different vesicles) performed the same day. See the Experimental Section and Table 1 for other details.

fitting analysis of NBD-PE fluorescence recovery kinetics after bleach (Figure 4) provides a diffusion coefficient of ~2.4 × 10^{-10} cm^2 s^{-1} with a very low mobile fraction (~15%) in gel phase membranes (see Table 1). The low mobile fraction of NBD-PE is apparent from the reduced fluorescence recovery

TABLE 1: Diffusion Parameters of NBD-Labeled Lipids in Gel Phase DPPC Membranes[a]

fluorescent probe	emission wavelength[b] (nm)	diffusion coeff[c] (10^{-10} cm^2 s^{-1})	mobile fract (%)[d]	N
NBD-PE	505−558	2.4 ± 0.3[e]	15 ± 1	15
25-NBD-cholesterol	505−558	3.8 ± 0.4[e]	88 ± 2	36
	505−526	4.9 ± 0.3[f]	89 ± 2	36
	537−558	3.7 ± 0.2[f]	74 ± 2	36

[a] Diffusion parameters were obtained from FRAP experiments at 23 °C on DPPC multilamellar vesicles that contained either 25-NBD-cholesterol or NBD-PE each at 1 mol % concentration as described in Materials and Methods. [b] Represents the range of wavelength in the fluorescence emission spectrum between which intensity was collected for FRAP experiments. [c] Diffusion coefficients were obtained from FRAP experiments carried out as described in Materials and Methods. The data represent means ± standard errors of N independent experiments. [d] The data represent means ± standard errors of N independent experiments. [e] These values are different at $P < 0.05$. [f] These values are different at $P < 0.01$.

into the bleached region (region 1 in Figure 3) even after a postbleach duration of ∼2 min.

Earlier reports on diffusion of fluorescent lipid probes monitored using FRAP in well-annealed gel phase multibilayers and supported membranes have suggested that the fluorescence recovery in such membranes is contributed by at least two populations of probes exhibiting different diffusion characteristics.[30,34−38] The slow ($\leq 10^{-11}$ cm^2 s^{-1}) component is believed to represent probe diffusion in the bulk of gel phase membrane whereas the relatively fast ($\sim 10^{-10}$ cm^2 s^{-1}) component could represent probe diffusion in sub-microscopic linear defects formed at the interstices of relatively homogeneous gel phase regions of the membrane. Such defects are believed to be intrinsic to the gel phase membrane organization and not experimentally induced artifacts.[30,34−37] In addition, such organization in gel phase membranes has been observed in freeze-fracture micrographs[39] and inferred from small-angle neutron scattering[40] and fluorescence energy transfer[41] experiments. The regions of defects are characterized by greater disorder and enhanced molecular diffusion rates.[30,35,41] In the present case, the estimated diffusion coefficient of $\sim 2.4 \times 10^{-10}$ cm^2 s^{-1} could represent mobility of NBD-PE molecules in such defects in the gel phase membrane. Interestingly, the fraction of molecules exhibiting such mobility is rather low (∼15%). Although a correlation between the mobile fraction and the actual concentration of a fluorescent probe in different environments (e.g., in the bulk gel phase and in defects) would be strictly valid only if it exhibits similar fluorescence intensities (quantum yields) in such environments, a possible reason for such a low mobile fraction could be the low abundance of NBD-PE in defect regions and preferential partitioning into the bulk of the gel phase membrane. Due to the slow diffusion rates ($\leq 10^{-11}$ cm^2 s^{-1}) of molecules in the bulk of the gel phase membrane, NBD-PE present in these regions of the membrane would appear immobile in the time scale of the present FRAP experiments. Further, masking of the possible presence of NBD-PE molecules in the defect regions due to self-quenching (and therefore an underestimation of its mobile fraction) can be ruled out since one would then have seen an abrupt increase in its fluorescence immediately following photobleaching in FRAP experiments, which is not the case (see Figure 3).

Similar experiments performed with 25-NBD-cholesterol in gel phase DPPC membranes showed a markedly different result. As shown in Figure 5, the fluorescence emission spectrum of 25-NBD-cholesterol in multilamellar vesicles appears smooth when the 25-NBD-cholesterol concentration is extremely low (0.1 mol %) with the maximum of fluorescence emission centered at 522 nm, as reported earlier.[16] An increase in the concentration of 25-NBD-cholesterol from 0.1 to 1 mol % leads to broadening of the fluorescence spectra with the gradual buildup of a new population which displays an emission peak at 544 nm (Figure 5). We have previously attributed the concentration-dependent shift in fluorescence emission and the

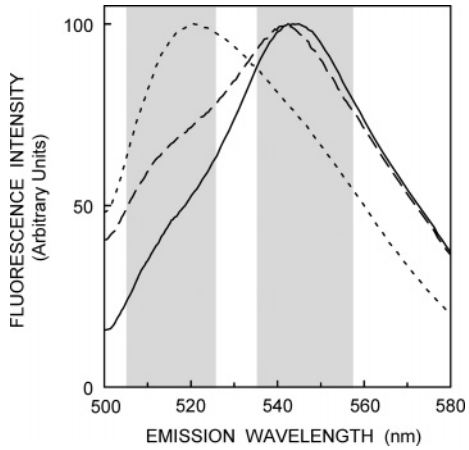

Figure 5. Fluorescence emission spectrum of 25-NBD-cholesterol in multilamellar vesicles of DPPC in the gel phase. The concentration of DPPC was 300 μM in all cases, whereas the concentrations of 25-NBD-cholesterol in the samples were 0.3 (0.1 mol %, ---), 1.5 (0.5 mol %, − − −), and 3 (1 mol %, —) μM. The excitation wavelength was 488 nm. The spectra are intensity-normalized at the respective emission maxima. The shaded portions of the spectra represent the two wavelength ranges (505−526 and 537−558 nm) from which fluorescence emission of 25-NBD-cholesterol was acquired for FRAP experiments as described in Figure 7. See the Experimental Section for other details.

concomitant spectral heterogeneity of 25-NBD-cholesterol to the formation of transbilayer tail-to-tail dimers of 25-NBD-cholesterol in the membrane[16,17] (see Figure 1b and later). The spectral features obtained with 1 mol % 25-NBD-cholesterol therefore correspond to the presence of both monomers and dimers of 25-NBD-cholesterol. Similar to the experiments performed with NBD-PE, diffusion characteristics of 25-NBD-cholesterol in gel phase DPPC membranes was monitored by FRAP experiments on multilamellar vesicles containing 1 mol % 25-NBD-cholesterol with the fluorescence emission acquired across the entire spectrum of 25-NBD-cholesterol (505−558 nm). This would provide a diffusion coefficient of 25-NBD-cholesterol that would reflect mobility of both monomers and transbilayer dimers of 25-NBD-cholesterol averaged over their respective quantum yields (fluorescence). As shown in Figure 6a, multilamellar vesicles containing 25-NBD-cholesterol appear large and uniformly fluorescent when observed under the confocal microscope. In this case also, the scanning parameters were optimized to ensure no appreciable fluorescence photobleaching during the measurement (see Figure 6b). Interestingly, nonlinear curve fitting analysis of fluorescence recovery kinetics after bleach (Figure 7a) shows that 25-NBD-cholesterol displays markedly different diffusion characteristics compared to NBD-PE in gel phase DPPC membranes. Thus, 25-NBD-cholesterol displays a significantly (∼1.6 fold) higher mobility than NBD-PE with a diffusion coefficient of $\sim 3.8 \times 10^{-10}$ cm^2 s^{-1} (see Table 1). More importantly, 25-NBD-cholesterol exhibits a

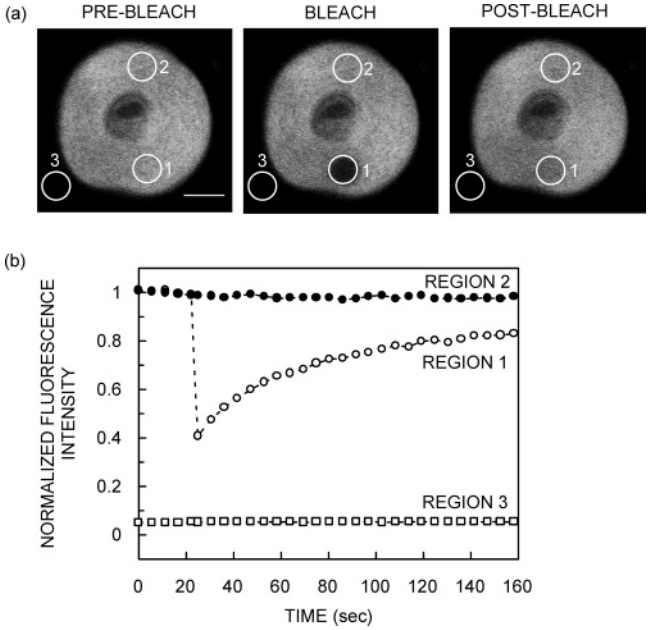

Figure 6. Representative FRAP experiment performed on a DPPC multilamellar vesicle containing 25-NBD-cholesterol. Panel a represents confocal sections of a DPPC multilamellar vesicle containing 25-NBD-cholesterol at 1 mol % concentration. The excitation wavelength was 488 nm, and fluorescence emission was collected from 505 to 558 nm. Fluorescence images of the same vesicle were acquired before bleach (prebleach), immediately after bleach (bleach), and after recovery of fluorescence (postbleach). The circular region 1 represents the bleached spot, region 2 reports fluorescence intensity outside the bleached spot but within the vesicle, and region 3 reports background fluorescence intensity. Panel b represents fluorescence intensity in the regions indicated in panel a over the entire time period of the FRAP experiment. Data corresponding to the mean normalized fluorescence intensity in regions 1−3 of panel a are represented in panel b. The mean fluorescence intensities represented in panel b have been normalized to the prebleach intensities in the respective region of interest and to the intensity in region 1. The constant fluorescence intensity in region 2 indicates no appreciable photobleaching in the field due to repeated imaging. The scale bar represents 5 μm. See the Experimental Section for other details.

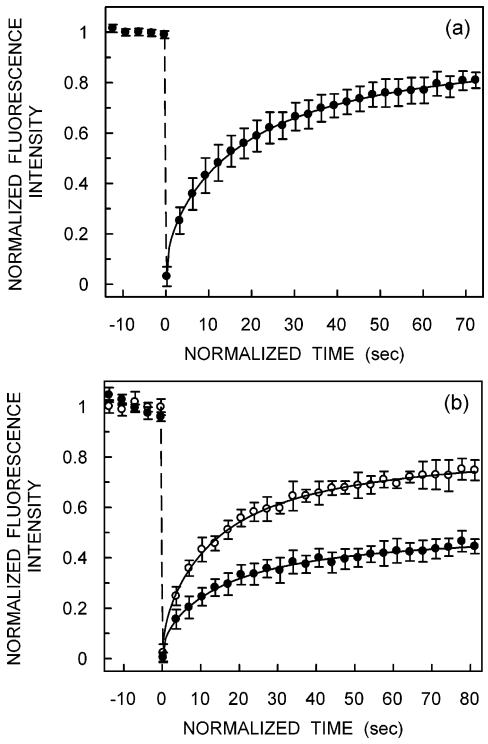

Figure 7. FRAP recovery kinetics of 1 mol % 25-NBD-cholesterol in DPPC multilamellar veisicles. Panel a shows the fluorescence recovery of 25-NBD-cholesterol with fluorescence emission collected from 505 to 558 nm. Panel b shows the wavelength-selective FRAP of 25-NBD-cholesterol in DPPC multilamellar vesicles where fluorescence emission was collected from 505 to 526 (○) and 537−558 (●) nm. The normalized prebleach intensities are shown at time $t < 0$. The solid lines are nonlinear regression fits to the data using eq 1. The data represent means ± standard deviations of several independent experiments (on different vesicles) performed on the same day. See the Experimental Section, Figure 5, and Table 1 for other details.

significantly higher mobile fraction (∼88%) than that of NBD-PE (∼15%). On the basis of the model of anomalous diffusion behavior of molecules in gel phase membranes (see above), it is possible that 25-NBD-cholesterol preferentially partitions into the region of defects in gel phase DPPC membranes thereby contributing to a relatively high mobile fraction.

The lateral mobility of molecules that are of dimensions similar to those of lipids has been described by the free area theory.[30,43,44] The free area theoretical framework is a semiempirical approach based on statistical mechanical considerations of density fluctuations in the lipid bilayer. According to this theory, transient voids that are created in the lipid bilayer by such density fluctuations are filled by the movement of neighboring lipid molecules into the void. This results in a type of diffusion that is independent of the hydrophobic thickness of the membrane and the cross-sectional area of the hydrophobic region of the diffusing molecule. However, the free area theory appears to be valid only for diffusion of small molecules in membranes that exist in the fluid phase. In the gel phase, however, it has been observed that small molecules do tend to display size-dependent lateral mobility. This has been attributed to the enhanced order in gel phase membranes that imposes constraints on displacement of molecules.[30] For instance, while the lateral mobilities of NBD-labeled alcohols of varying sizes were found to be similar in fluid phase membranes in FRAP measurements, the same molecules displayed size-dependent mobilities in gel phase membranes.[30] In the present case, the higher mobility of 25-NBD-cholesterol compared to NBD-PE could therefore be due to the smaller molecular size of cholesterol compared to that of phospholipid (see later). It must be mentioned here that mobility of a headgroup-labeled fluorescent cholesterol analogue has previously been reported to be higher than a fluorescent phospholipid analogue only in gel phase membranes.[31]

The concentration-dependent shift in fluorescence emission spectra of 25-NBD-cholesterol in gel phase DPPC vesicles has been reported earlier.[16,17] Experiments carried out with unilamellar DPPC vesicles in the gel phase showed that, at very low concentrations (0.1 mol %), the fluorescence emission spectrum of 25-NBD-cholesterol is homogeneous with the maximum of fluorescence emission at 522 nm, which corresponds to the spectral feature of the 25-NBD-cholesterol monomers in the membrane. With an increase in concentration, the emission spectrum of 25-NBD-cholesterol becomes broad with the appearance of a new emission maximum at ∼541 nm. We have earlier proposed concentration-dependent transbilayer organization of dimers of 25-NBD-cholesterol molecules which alters the emission properties of the NBD group thereby resulting in the appearance of the emission maximum at ∼541 nm. It is important to mention here that the absorption spectrum of 25-NBD-cholesterol also exhibits such concentration-dependent characteristics indicating that the organization of 25-NBD-cholesterol as a transbilayer assembly is not an excited-state phenomenon of the NBD group but reflects ground-state

heterogeneity of the cholesterol analogue.[16] Interestingly, we have recently shown that the microenvironment around the NBD group in the dimer arrangement is more rigid and constrained than that of the monomer as evidenced by red edge excitation shift studies.[19] This microenvironmental restriction in the dimer could be generated due to the definite spatial orientation of the two NBD groups in the dimer arrangement resulting in steric constraints.

The concentration-dependent spectral features of 25-NBD-cholesterol (shift in fluorescence emission maximum toward longer wavelengths) is reproduced in multilamellar vesicles of DPPC (Figure 5). If 25-NBD-cholesterol indeed exhibits such an organization in gel phase DPPC membranes, the transbilayer assembly would be larger in size compared to monomers and would be expected to display different diffusion properties. The differences in the diffusion properties of the two populations of 25-NBD-cholesterol could be analyzed by FRAP experiments performed either by varying the concentration of 25-NBD-cholesterol in the membrane or by photoselecting these populations at a fixed concentration of 25-NBD-cholesterol. We chose to adopt the latter strategy since (i) wavelength-selective FRAP experiments would represent a convenient method to photoselect the two populations of 25-NBD-cholesterol that exist in equilibrium, (ii) such experiments would involve monitoring diffusion properties of 25-NBD-cholesterol present at a given concentration thereby avoiding any possible complications (heterogeneity) arising due to changes in physical properties of the membranes upon addition of increasing concentrations of 25-NBD-cholesterol, and (iii) it has been difficult to perform concentration-dependent FRAP experiments at low concentrations (<1 mol %) of 25-NBD-cholesterol due to the low signal-to-noise ratio.

Wavelength-selective FRAP experiments were carried out under conditions similar to those described earlier (see Figure 6) but with the fluorescence emission collected from a wavelength range of 505−526 and 537−558 nm simultaneously to photoselect 25-NBD-cholesterol molecules. These wavelength ranges are shown as shaded portions in the emission spectra of 25-NBD-cholesterol in Figure 5. Nonlinear curve fits of the fluorescence recovery kinetics from such experiments are shown in Figure 7b, and the diffusion parameters obtained from such fits are shown in Table 1. Such analysis indicates that the two populations indeed display significantly different diffusion properties. The population emitting at a shorter wavelength range (505−526) displays a ∼1.3-fold higher mobility than that emitting at a longer wavelength range (537−558) (see Table 1). In addition, both populations display a higher mobile fraction than that of NBD-PE possibly indicating that they both preferentially localize in defect regions in gel phase DPPC membranes. Moreover, these results indicate that fluorescence recovery kinetics of 25-NBD-cholesterol obtained from FRAP experiments where the fluorescence from the entire emission spectrum of 25-NBD-cholesterol (505−558 nm) was considered (Figure 7a) must reflect mobility of at least two populations of 25-NBD-cholesterol averaged over their respective quantum yields (fluorescence). It should be kept in mind that the diffusion coefficient of 25-NBD-cholesterol estimated from FRAP measurements where fluorescence from the entire emission spectrum (505−558 nm) was collected (see Table 1) would depend on the relative mobility and fluorescence quantum yield of these two populations. In general, fluorescence recovery kinetics would predominantly reflect diffusion of the faster moving population and the population having higher quantum yield (fluorescence). The situation is somewhat complicated here since the faster moving population (predominantly monomers of 25-NBD-cholesterol) is characterized by lower intrinsic fluorescence (see Figure 5). This could explain our observation that the estimated diffusion parameters of 25-NBD-cholesterol obtained when fluorescence was collected from the wavelength range of 505−558 nm is closer to that obtained when the emission was collected from 537 to 558 nm. Nevertheless, our results show that mobility of 25-NBD-cholesterol is higher compared to that of NBD-PE irrespective of the wavelength range at which emission of 25-NBD-cholesterol is acquired (see Table 1). As a control, we performed a similar wavelength-selective FRAP experiment on NBD-PE to determine if diffusion parameters obtained from such measurements are generally affected by the wavelength at which fluorescence emission is collected. The diffusion parameters of NBD-PE obtained when fluorescence emission is collected from a wavelength range 505−526 nm ($D = (2.6 \pm 0.1) \times 10^{-10}$ cm^2 s^{-1} and $R = 19 \pm 1\%$) are not significantly different from those obtained at a wavelength range 537−558 nm ($D = (2.5 \pm 1.1) \times 10^{-10}$ cm^2 s^{-1} and $R = 17 \pm 1\%$). These results suggest that diffusion parameters of NBD-cholesterol obtained from wavelength-selective FRAP measurements do not reflect an intrinsic dependence of diffusion parameters on the range of wavelengths used to collect fluorescence emission but indicate the presence of distinct populations of NBD-cholesterol with different mobilities.

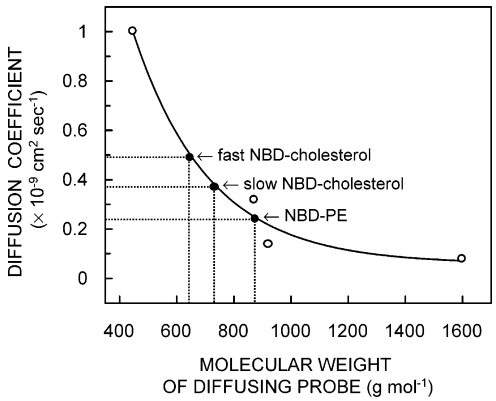

Figure 8. Dependence of the diffusion coefficient of the probe on its size in gel phase membranes. The figure shows diffusion coefficients of a series of probes in gel phase membranes plotted against their respective molecular weights. Diffusion coefficients of the probes (open circles) are from Balcom and Petersen (1993).[30] Data (open circles) on diffusion coefficients of probes and their respective molecular weights were fit to the equation, $y = ae^{(-bx)} + c$, and the fit results provide estimates for the constants $a = 5.0359$, $b = 0.0038$, and $c = 0.0592$. These estimates and the experimentally obtained diffusion coefficients of NBD-PE and the fast- and slow-diffusing populations of 25-NBD-cholesterol were plugged in the above equation (closed circles) to obtain empirical estimates of their respective molecular weights. See text for other details.

If the mobility of molecules in gel phase membranes is dependent on the size of the molecule, as has been earlier observed for NBD-labeled alcohols,[30] such data could set up an empirical scale for determining the effective molecular size of the two populations of 25-NBD-cholesterol. We used the data reported by Balcom and Petersen (1993)[30] to generate a plot of the diffusion coefficients of probes vs their respective molecular weights (see Figure 8). Interestingly, such a plot appears to follow an exponential form such that the difference between diffusion coefficients of probes is pronounced in the low molecular weight range. As shown in Figure 8, data on the diffusion coefficients of probes vs their molecular weights could be fitted well ($r^2 = 0.98$) to an exponential decay function with

an offset (see Figure 8 and the accompanying legend). To analyze the validity of such an approach to predict the molecular weight of the diffusing probe from its diffusion coefficient, we derived the molecular weight of NBD-PE by utilizing its experimentally obtained diffusion coefficient (Table 1). Importantly, the molecular weight of NBD-PE derived from such analysis is 876 g mol^{-1}, which is in excellent agreement with its actual molecular weight of 872.1 g mol^{-1}. The close similarity between the derived and actual molecular weights of NBD-PE ensures that this approach is valid for estimating the molecular weights of the fast- and slow-diffusing populations of 25-NBD-cholesterol from the experimentally obtained diffusion coefficients at two emission wavelengths (505−526 and 537−558 nm). Such analysis indicates that the fast-diffusing population of 25-NBD-cholesterol has an effective molecular weight of 647 g mol^{-1} whereas the slow-diffusing population has an effective molecular weight of 733 g mol^{-1}, while the actual molecular weight of 25-NBD-cholesterol is 564.7 g mol^{-1}. These estimates suggest that the fast-diffusing population could comprise of 25-NBD-cholesterol that predominantly exist as monomers, whereas the slow-diffusing population could have a significant proportion of dimers of 25-NBD-cholesterol.

It is important to mention here that the two wavelength ranges used to collect fluorescence emission of 25-NBD-cholesterol (Figure 5) are not mutually exclusive; i.e., the separation of two diffusing populations of 25-NBD-cholesterol on the basis of these two wavelength ranges is not complete. This is due to the fact that fluorescence spectra in solutions (more so in microheterogeneous dispersions such as membranes) are always broad and any assignment of an emission maximum to a given excited-state species could at best be approximate. The kinetics of fluorescence recovery of 25-NBD-cholesterol may not therefore exclusively reflect the mobility of these two populations of 25-NBD-cholesterol (monomers and dimers) when fluorescence emission is acquired using these two wavelength ranges. It is therefore possible that the derived molecular weights of the fast- and slow-diffusing populations of 25-NBD-cholesterol may not exactly correspond to those of a monomer and dimer of 25-NBD-cholesterol but represent informative estimates.

Discussion

In this paper, we have utilized FRAP to address the spatial organization and dynamics of 25-NBD-cholesterol in the membrane at low concentrations. Our results on the diffusion properties of 25-NBD-cholesterol and NBD-PE can be rationalized on the basis of a model that depicts the distribution of these two fluorescent analogues in gel phase membranes. Figure 9a shows a two-dimensional representation of a gel phase bilayer composed of DPPC molecules which adopt a tilted orientation with respect to the plane of the bilayer and where the fatty acyl chains are parallel to each other, as has been inferred from X-ray diffraction studies.[45] The same bilayer is represented as a three-dimensional membrane in Figure 9b. Membranes composed of DPPC molecules oriented in this manner represent well-packed membrane regions (shown in blue) that are characterized by high degree of order and low lateral mobility ($\leq 10^{-11}$ cm^2 s^{-1}).[30,37,38] The boundary between two well-packed membranes formed of DPPC molecules arranged in opposite orientation could represent regions that display packing defects (shown in yellow). Such regions may possess relatively fluidlike characteristics with lower degree of order and high lateral mobility ($\sim 10^{-10}$ cm^2 s^{-1}). The membrane in the gel phase is therefore assumed to be intrinsically heterogeneous with the presence of at least two environments that display markedly different dynamics. The matching lengths of the fatty acyl chains of NBD-PE and that of the host membrane would favor partitioning of NBD-PE into the well-packed and homogeneous gel phase membrane regions (shown in blue) that display reduced lateral mobility. When monitored for a limited duration of time, such reduced mobility would manifest in a reduced mobile fraction in FRAP experiments, similar to what is observed in the present case (see Table 1). On the contrary, due to the structural differences between the cholesterol analogue and DPPC, most of 25-NBD-cholesterol would be expected to partition into the defect regions of the membrane resulting in a higher mobile fraction in FRAP experiments. Spectroscopic measurements have earlier shown that 25-NBD-cholesterol molecules could exist as transbilayer tail-to-tail dimers (shown in Figures 1b and 9) that display fluorescence emission characteristics distinct from those of 25-NBD-cholesterol monomers.[16,17,19] We propose that the presence of fast- and slow-diffusing populations of 25-NBD-cholesterol (see Table 1) could correspond to predominant populations of monomers and dimers of 25-NBD-cholesterol, respectively (Figure 9). In addition, both these populations display high mobile fractions possibly reflecting their localization in regions of defects in gel phase membrane.

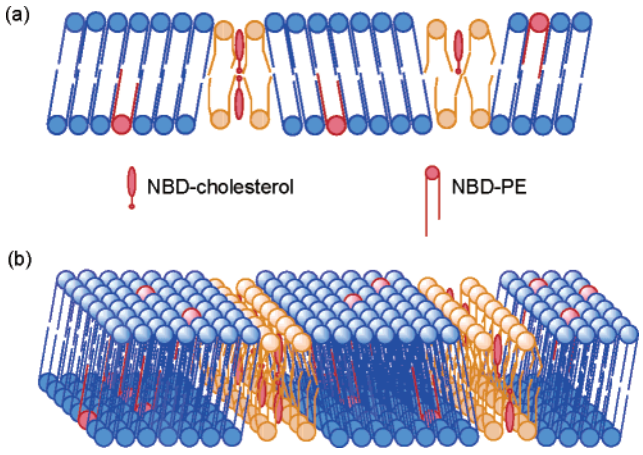

Figure 9. Schematic representation depicting the distribution of NBD-PE and 25-NBD-cholesterol in gel phase DPPC membranes. Panel a shows a two-dimensional representation of a gel phase bilayer composed of DPPC molecules. Panel b is a three-dimensional representation of the same membrane. The DPPC molecules predominantly adopt a tilted orientation with respect to the plane of the bilayer and have their fatty acyl chains arranged parallel to each other. Such regions (shown in blue) represent well-packed membrane regions which are characterized by high degree of order and low lateral mobility. The boundary between two well-packed membranes formed of DPPC molecules arranged in opposite orientation could represent regions that display packing defects (shown in yellow). Such regions possess relatively fluidlike characteristics with lower degree of order and high lateral mobility. The remarkably different mobile fractions of NBD-PE and 25-NBD-cholesterol in such membranes (see Table 1) suggest preferential partitioning of NBD-PE into the blue ordered regions and 25-NBD-cholesterol into the yellow disordered regions in the membrane. On the basis of the heterogeneity in the fluorescence emission spectra in gel phase DPPC membranes, 25-NBD-cholesterol has been proposed to exhibit transbilayer tail-to-tail dimers that coexist with monomers[3,22] (see Figure 1b). Our present results from wavelength-selective FRAP experiments (see Table 1) suggest the presence of at least two populations of 25-NBD-cholesterol that exhibit significantly different diffusion properties and could correspond to predominant populations of monomers and dimers of 25-NBD-cholesterol. See text for further details.

In summary, we report here a novel wavelength-selective FRAP approach that distinguishes subpopulations of diffusing fluorescent molecules on the basis of differences in their

fluorescence emission properties. This method can in principle be utilized in diffusion-based measurements to monitor the organization and dynamics of other membrane constituents labeled with fluorescent probes that exhibit shifted emission spectra depending on their aggregation state and microenvironments in membranes. The cholesterol analogue 25-NBD-cholesterol displays such concentration-dependent spectral characteristics which has been utilized in wavelength-selective FRAP experiments in the present case to monitor its organization and dynamics at low concentrations in gel phase membranes. The ability to detect different diffusing populations using FRAP (which in the present experiments measures diffusion in the time scale of seconds) further suggests intrinsic heterogeneity of this analogue in gel phase membranes. The application of the wavelength-selective FRAP approach to understand the organization and dynamics of fluorescently labeled membrane constituents that display concentration- and/or extrinsic cofactor-dependent alterations in their fluorescence emission properties while existing in an intact cellular environment represents an exciting possibility.

Acknowledgment. This work was supported by the Council of Scientific and Industrial Research, Government of India. T.J.P. and S.M. thank the Council of Scientific and Industrial Research for the award of Senior Research Fellowships. A.C. is an Honorary Professor of the Jawaharlal Nehru Centre for Advanced Scientific Research, Bangalore, India. We thank Nandini Rangaraj, V. K. Sarma, N. R. Chakravarthi, and K. N. Rao for technical help with confocal microscopy. We thank members of our laboratory for critically reading the manuscript.

References and Notes

(1) Schroeder, F.; Woodford, S. S.; Kavecansky, J.; Wood, W. G.; Joiner, C. *Mol. Membr. Biol.* **1995**, *12*, 113.
(2) Mouritsen, O. G.; Zuckermann, M. J. *Lipids* **2004**, *39*, 1101.
(3) Emoto, K.; Kobayashi, T.; Yamaji, A.; Aizawa, H.; Yahara, I.; Inoue, K.; Umeda, M. *Proc. Natl. Acad. Sci. U.S.A.* **1996**, *93*, 12867.
(4) Ostrowski, S. G.; Van Bell, C. T.; Winograd, N.; Ewing, A. G. *Science* **2004**, *305*, 71.
(5) Gambhir, A.; Hangyás-Mihályné, G.; Zaitseva, I.; Cafiso, D. S.; Wang, J.; Murray, D.; Pentyala, S. N.; Smith, S. O.; McLaughlin, S. *Biophys. J.* **2004**, *86*, 2188.
(6) Simons, K.; Toomre, D. *Nat. Rev. Mol. Cell Biol.* **2000**, *1*, 31.
(7) McLaughlin, S.; Wang, J.; Gambhir, A.; Murray, D. *Annu. Rev. Biophys. Biomol. Struct.* **2002**, *31*, 151.
(8) Lagerholm, B. C.; Weinreb, G. E.; Jacobson, K.; Thompson, N. L. *Annu. Rev. Phys. Chem.* **2005**, *56*, 309.
(9) Schroeder, F. *Prog. Lipid Res.* **1984**, *23*, 97.
(10) Grechishnikova, I. V.; Bergstrom, F.; Johansson, L. B.-A.; Brown, R. E.; Molotkovsky, J. G. *Biochim. Biophys. Acta* **1999**, *1420*, 189.
(11) Pagano, R. E.; Chen, C. S. *Ann. N.Y. Acad. Sci.* **1998**, *845*, 152.
(12) Chattopadhyay, A. *Chem. Phys. Lipids* **1990**, *53*, 1.
(13) Koval, M.; Pagano, R. E. *J. Cell Biol.* **1990**, *111*, 429.
(14) Chattopadhyay, A.; London, E. *Biochemistry* **1987**, *26*, 39.
(15) Chattopadhyay, A.; London, E. *Biochim. Biophys. Acta* **1988**, *938*, 24.
(16) Mukherjee, S.; Chattopadhyay, A. *Biochemistry* **1996**, *35*, 1311.
(17) Rukmini, R.; Rawat, S. S.; Biswas, S. C.; Chattopadhyay, A. *Biophys. J.* **2001**, *81*, 2122.
(18) Kelkar, D. A.; Chattopadhyay, A. *J. Phys. Chem. B* **2004**, *108*, 12151.
(19) Mukherjee, S.; Chattopadhyay, A. *Chem. Phys. Lipids* **2005**, *134*, 79.
(20) Mitra, B.; Hammes, G. G. *Biochemistry* **1990**, *29*, 9879.
(21) Harris, J. S.; Epps, D. E.; Davio, S. R.; Kezdy, F. R. *Biochemistry* **1995**, *34*, 3851.
(22) Loura, L. M. S.; Prieto, M. *Biophys. J.* **1997**, *72*, 2226.
(23) Jacobson, K.; Sheets, E. D.; Simson, R. *Science* **1995**, *268*, 1441.
(24) Kusumi, A.; Nakada, C.; Ritchie, K.; Murase, K.; Suzuki, K.; Murakoshi, H.; Kasai, R. S.; Kondo, J.; Fujiwara, T. *Annu. Rev. Biophys. Biomol. Struct.* **2005**, *34*, 351.
(25) Scheidt, H. A.; Müller, P.; Herrmann, A.; Huster, D. J. *J. Biol. Chem.* **2003**, *278*, 45563.
(26) Shaw, J. E.; Epand, R. F.; Epand, R. M.; Li, Z.; Bittman, R.; Yip, C. M. *Biophys. J.* **2006**, *90*, 2170.
(27) McClare, C. W. F. *Anal. Biochem.* **1971**, *39*, 527.
(28) Haugland, R. P. In *Handbook of Fluorescent Probes and Research Chemicals*, 6th ed.; Molecular Probes Inc.: Eugene, OR, 1996.
(29) Soumpasis, D. M. *Biophys. J.* **1986**, *41*, 95.
(30) Balcom, B. J.; Petersen, N. O. *Biophys. J.* **1993**, *65*, 630.
(31) Alecio, M. R.; Golan, D. E.; Veatch, W. R.; Rando, R. R. *Proc. Natl. Acad. Sci. U.S.A.* **1982**, *79*, 5171.
(32) Golan, D. E.; Alecio, M. R.; Veatch, W. R.; Rando, R. R. *Biochemistry* **1984**, *23*, 332.
(33) Chattopadhyay, A.; Mukherjee, S. *Biochemistry* **1993**, *32*, 3804.
(34) Wu, E.-S.; Jacobson, K.; Papahadjopoulos, D. *Biochemistry* **1977**, *16*, 3936.
(35) Derzko, Z.; Jacobson, K. *Biochemistry* **1980**, *19*, 6050.
(36) Schneider, M. B.; Chan, W. K.; Webb, W. W. *Biophys. J.* **1983**, *43*, 157.
(37) Bultmann, T.; Vaz, W. L. C.; Melo, E. C. C.; Sisk, R. B.; Thompson, T. E. *Biochemistry* **1991**, *30*, 5573.
(38) Crane, J. M.; Tamm, L. K. *Biophys. J.* **2004**, *86*, 2965.
(39) Meyer, H. W.; Richter, W. *Micron* **2001**, *32*, 615.
(40) Gordeliy, V. I.; Ivkov, V. G.; Ostanevich, Y. M.; Yaguzhinskij, L. S. *Biochim. Biophys. Acta* **1991**, *1061*, 39.
(41) Loura, L. M. S.; Fedorov, A.; Prieto, M. *Biophys. J.* **1996**, *71*, 1823.
(42) Kapitza, H. G.; Ruppel, D. A.; Galla, H.-J.; Sackmann, E. *Biophys. J.* **1984**, *45*, 577.
(43) Vaz, W. L. C.; Hallman, D. *FEBS Lett.* **1983**, *152*, 287.
(44) Vaz, W. L. C.; Clegg, R. M.; Hallmann, D. *Biochemistry* **1985**, *24*, 781.
(45) Nagle, J. F.; Tristram-Nagle, S. *Biochim. Biophys. Acta* **2000**, *1469*, 159.